New Journal of Physics
The open access journal at the forefront of physics

Deutsche Physikalische Gesellschaft DPG IOP Institute of Physics

PAPER • OPEN ACCESS

Mean first-passage time to a small absorbing target in an elongated planar domain

To cite this article: Denis S. Grebenkov and Alexei T. Skvortsov 2020 *New J. Phys.* **22** 113024

New Journal of Physics
The open access journal at the forefront of physics

Deutsche Physikalische Gesellschaft DPG
IOP Institute of Physics

Published in partnership with: Deutsche Physikalische Gesellschaft and the Institute of Physics

CrossMark

OPEN ACCESS

RECEIVED
18 September 2020

REVISED
24 October 2020

ACCEPTED FOR PUBLICATION
10 November 2020

PUBLISHED
23 November 2020

PAPER

Mean first-passage time to a small absorbing target in an elongated planar domain

Denis S. Grebenkov[1,*] **and Alexei T. Skvortsov**[2]

[1] Laboratoire de Physique de la Matière Condensée (UMR 7643), CNRS–Ecole Polytechnique, IP Paris, 91128 Palaiseau, France
[2] Maritime Division, Defence Science and Technology, 506 Lorimer Street, Fishermans Bend, Victoria 3207, Australia
[*] Author to whom any correspondence should be addressed.

E-mail: denis.grebenkov@polytechnique.edu

Keywords: diffusion, first-passage time, homogenisation, reactivity, elongated domain

Abstract

We derive an approximate but fully explicit formula for the mean first-passage time (MFPT) to a small absorbing target of arbitrary shape in a general elongated domain in the plane. Our approximation combines conformal mapping, boundary homogenisation, and Fick–Jacobs equation to express the MFPT in terms of diffusivity and geometric parameters. A systematic comparison with a numerical solution of the original problem validates its accuracy when the starting point is not too close to the target. This is a practical tool for a rapid estimation of the MFPT for various applications in chemical physics and biology.

1. Introduction

The concept of first-passage time (FPT) is ubiquitous in describing phenomena around us. Being originally stemmed from the theory of Brownian motion as a time taken for a diffusing particle to arrive at a given location, nowadays it is widely used in chemistry (geometry-controlled kinetics), biology (gene transcription, foraging behaviour of animals) and many applications (financial modelling, forecasting of extreme events in the environment, time to failure of complex devices and machinery, military operations). This subject has an extensive literature, see [1–15] and references therein. There is also a rich variety of different physical phenomena that can be analytically treated with the framework of the FPT due to similarity of underlying equations [16].

In a basic setting, the first-passage problem is formulated in the following way. We consider a Brownian particle initially located at point $\mathbf{r}$ of a bounded domain Ω and searching for a small target $\mathcal{S}$ (a small region with absorbing boundary) inside that domain (if the target is at the boundary the problem is usually referred to as the narrow escape problem [9]). As the first-passage time of the particle to the target is a random variable, its full characterisation requires the computation of its distribution [17–24]. In many practical situations, however, it is enough to estimate the average time $T(\mathbf{r})$ taken for the particle to hit the target (see [1, 3, 4, 25–28] and references therein). The mean first-passage time (MFPT) satisfies the Poisson equation [1]

$$D\Delta T(\mathbf{r}) = -1, \tag{1}$$

where D is the particle diffusivity, and Δ is the Laplace operator. The boundary of the domain is assumed reflecting, $\partial T/\partial n = 0$ on $\mathbf{r} \in \partial\Omega$ (with $\partial/\partial n$ being the normal derivative) and the target surface is absorbing, $T = 0$ on $\mathbf{r} \in \partial\mathcal{S}$.

In spite of an apparent simplicity of equation (1) and a variety of powerful methods for its analysis, to date the exact closed-form solutions of equation (1) are available only for a few special cases and for the domains with high symmetry such as a sphere or a disk [1]. Many approximate solutions, derived by advanced asymptotic methods, can produce a remarkable agreement with numerical solutions of equation (1), but often require specific mathematical expertise and still involve some level of numerical treatment [3, 4, 8–10, 29–37]. This necessitates the development of analytical approximations that being

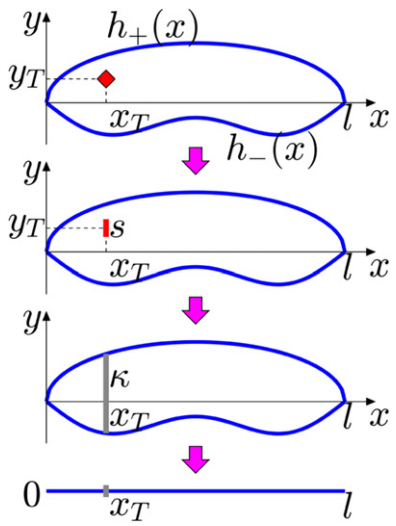

Figure 1. Three-step transformation of the original MFPT problem into an effectively one-dimensional problem with semi-permeable semi-absorbing boundary condition.

perhaps less accurate can lead to simple explicit expressions that provide reasonable estimations for MFPT in some general geometric settings. This was one of the main motivations for the present study.

The aim of the paper is to derive a general formula for the MFPT in an *elongated* planar domain with reflecting boundaries. The profile of the domain is assumed to be smooth, slowly changing, but otherwise general. The target is assumed to be small but of an arbitrary shape. We validate our findings by numerical solution of equation (1) via a finite elements method. Remarkably, this simple general formula, derived under a number of simplified approximations, turns out to be surprisingly accurate.

2. Approximation for the MFPT

We consider an elongated planar domain of 'length' l, which is determined by two smooth profiles $h_-(x) < h_+(x)$ (figure 1):

$$\Omega = \{(x, y) \in \mathbb{R}^2 \ : \ 0 < x < l, \ h_-(x) < y < h_+(x)\}. \tag{2}$$

In particular, the local 'width' of the domain is $h(x) = h_+(x) - h_-(x)$, and $h_0 = \max\{h(x)\}$ is the maximal width. Throughout the paper, we assume that the aspect ratio h_0/l of the domain is small. A small absorbing target (also called trap or sink) is located inside the domain at some (x_T, y_T), which is not too close to the boundary.

The main analytical formula will be derived by employing a three-step approximation. First, we replace the absorbing target by a vertical absorbing interval of the same conformal radius r_c, or the same trapping rate, or the same logarithmic capacity (since they all are proportional to each other [38]). Far away from the target such a replacement is justifiable since at the distance greater than the size of the target (but still much smaller than $h(x_T)$ and l) the absorption flux can be characterised by the first (monopole) moment of the shape of the target, and this equivalence preserves it. For a variety of planar shapes (circle, ellipse, arc, triangle, square, or even some fractals [39, 40]), the conformal radius is well-known or can be accurately estimated from various approximations, see [12, 38, 40] and references therein. For instance, for an elliptical target with semi-axes a and b, its conformal radius is $r_c = (a + b)/2$, so for an absorbing interval of length s conformal radius is simply $r_c = s/4$. As a consequence, the length of the equivalent absorbing interval for any target with the conformal radius r_c is given by $s = 4r_c$.

Second, we substitute the absorbing interval at $x = x_T$ by an equivalent semi-permeable semi-absorbing vertical boundary. In line with the conventional arguments of effective medium theory, the trapping effect of the target can approximately be captured by means of this boundary with an effective reactivity κ. More specifically, we assume that the trapping rate of this effective boundary is equal to the trapping flux of the particles induced by the presence of the target. The well-known examples of such an approach are acoustic impedance of perforated screens [41] and effective electric conductance of lattices and grids [42–44]. The effective reactivity can be related to the geometrical parameters by employing the ideas of boundary homogenisation [13, 43, 44]. In particular, an explicit form of this reactivity in the case of two absorbing arcs on the reflecting boundary of a disk of radius R was found in [13]. As shown in [13], an appropriate

conformal mapping allows one to transform such a disk into an infinite horizontal stripe of width $2h$ with reflecting boundary that includes two identical absorbing intervals. By symmetry, this domain is also equivalent to a twice narrower stripe (i.e., of width h) with a single absorbing interval with a prescribed offset with respect to the reflecting boundary. Upon these transformations, the original formula of the effective reactivity is preserved, except that the perimeter of the disk, $2\pi R$, is replaced by the stripe width:

$$\kappa = \frac{D}{h(x_T)} \frac{\pi}{\ln(1/F)}, \tag{3}$$

where

$$F = \sqrt{\sin^2\left[\frac{\pi}{2}(\sigma + \sigma_g)\right] - \sin^2\left(\frac{\pi}{2}\sigma_g\right)}, \tag{4}$$

with $\sigma = s/h(x_T)$ and $\sigma_g = (y_T - s/2)/h(x_T)$. Here, we used the width of the domain, $h(x_T)$, at the location of the target. Even though equation (3) was derived for an infinite stripe, it is also applicable for an elongated rectangle of width $h(x_T)$. Moreover, we will use it as a first approximation for general elongated domains.

Third, the Brownian particle, which is released at some point (x, y) inside an elongated domain, frequently bounces from the horizontal reflecting walls while gradually diffusing along the domain towards the target. The shape of the horizontal walls (defined by $h_\pm(x)$) can additionally create an entropic drift, which can either speed up or slow down the arrival to the target. In any case, the information about the particle initial location in the vertical direction, y, becomes rapidly irrelevant, and the original MFPT problem, equation (1), is reduced to a one-dimensional problem. While the classical Fick–Jacobs equation determines the concentration $c(x, t)$ averaged over the cross-section (see [45–50] and references therein), the survival probability is determined by the backward diffusion equation with the adjoint diffusion operator [51]. In particular, equation (1) in an elongated domain reduces to

$$\frac{D}{h(x)} \frac{\mathrm{d}}{\mathrm{d}x}\left[h(x)\frac{\mathrm{d}T(x)}{\mathrm{d}x}\right] = -1. \tag{5}$$

In summary, we transformed the original problem of finding the MFPT to a small target of arbitrary shape in a general elongated domain to the one-dimensional problem, which can be solved analytically.

We search for the solution of equation (5) in the intervals $(0, x_T)$ and (x_T, l). Multiplying this equation by $h(x)/D$, integrating over x and imposing Neumann (reflecting) boundary conditions at $x = 0$ and $x = l$, we get

$$T(x) = \begin{cases} C_- - \displaystyle\int_0^x \mathrm{d}x' \frac{S(x')}{Dh(x')} & (0 < x < x_T), \\ C_+ - \displaystyle\int_x^l \mathrm{d}x' \frac{S(l) - S(x')}{Dh(x')} & (x_T < x < l), \end{cases} \tag{6}$$

where $S(x) = \int_0^x \mathrm{d}x'\, h(x')$ is the area of (sub)domain restricted between 0 and x. The integration constants $C_\pm$ are determined by imposing the effective semi-permeable semi-absorbing boundary condition at the target location:

$$T(x_T - 0) = T(x_T + 0), \tag{7a}$$

$$D\left[\frac{\mathrm{d}T}{\mathrm{d}x}(x_T + 0) - \frac{\mathrm{d}T}{\mathrm{d}x}(x_T - 0)\right] = \kappa\, T(x_T). \tag{7b}$$

The first relation ensures the continuity of the MFPT, whereas the second condition states that the difference of the diffusive fluxes at two sides of the semi-permeable boundary at x_T is equal to the reaction flux on the target. The latter flux is proportional to $T(x_T)$, with an effective reactivity κ from equation (3).

Substituting equation (6) into equation (7), we get the final solution of the problem:

$$T(x) = \frac{l^2}{D}\left(U_{\sigma_x}(x_T/l) - U_{\sigma_x}(x/l)\right) + \frac{l}{\kappa}\frac{Y(1)}{y(x_T/l)}, \tag{8}$$

where $y(z)$ is the rescaled width profile, $h(x) = h_0 y(x/l)$ (with $z = x/l$), and

$$Y(z) = \int_0^z \mathrm{d}z'\, y(z'), \tag{9}$$

$$U_-(z) = \int_0^z \mathrm{d}z' \frac{Y(z')}{y(z')}, \quad U_+(z) = \int_z^1 \mathrm{d}z' \frac{Y(1) - Y(z')}{y(z')}. \tag{10}$$

Table 1. Several examples of symmetric elongated domains defined by setting $-h_-(x) = h_+(x) = \frac{1}{2}h(x) = \frac{1}{2}\,h_0\,y(x/l)$: the rescaled profile $y(z)$, its integral $Y(z)$, functions $U_\pm(z)$ from equation (10), the rescaled area $Y(1)$ (such that $S = lh_0Y(1)$), and the shape-dependent constant C_y from equation (15). For all domains, which are symmetric with respect to the vertical line at $l/2$, one has $U_+(z) = U_-(1-z)$.

Domain	$y(z)$	$Y(z)$	$U_-(z)$	$U_+(z)$	$Y(1)$	C_y
Rectangular	1	z	$\frac{1}{2}z^2$	$U_-(1-z)$	1	$\frac{1}{6}$
Triangular	z	$\frac{1}{2}z^2$	$\frac{1}{4}z^2$	$\frac{1}{4}(z^2-1-2\ \ln\ z)$	$\frac{1}{2}$	$\frac{1}{8}$
Rhombic	$1-\lvert 2z-1\rvert$	$\begin{cases} z^2 & (z<0.5) \\ \frac{1}{2}-(1-z)^2 & (z>0.5)\end{cases}$	$\begin{cases} \frac{1}{4}z^2 & (z<0.5) \\ \frac{(1-z)^2-\ln(2-2z)}{4} & (z>0.5)\end{cases}$	$U_-(1-z)$	$\frac{1}{2}$	$\frac{3}{32}$
Sinusoidal	$\sin(\pi z)$	$\frac{1}{\pi}(1-\cos(\pi z))$	$\frac{1}{\pi^2}\,(\ln\ 2-\ln(1+\cos(\pi z)))$	$U_-(1-z)$	$\frac{2}{\pi}$	$\frac{1}{\pi^2}$
Parabolic	$4z(1-z)$	$2z^2(1-2z/3)$	$\frac{1}{6}\left(z^2-z-\ln(1-z)\right)$	$U_-(1-z)$	$\frac{2}{3}$	$\frac{19}{180}$
Elliptic	$\sqrt{1-(2z-1)^2}$	$\frac{\pi}{8}+\frac{1}{4}\mathrm{asin}(2z-1)$ $-(\frac{1}{2}-z)\sqrt{z(1-z)}$	$\frac{\pi^2}{64}+\frac{z(z-1)}{4}+\frac{\mathrm{asin}^2(2z-1)}{16}$ $+\frac{\pi}{16}\mathrm{asin}(2z-1)$	$U_-(1-z)$	$\frac{\pi}{4}$	$\frac{\pi^2}{48}-\frac{5}{64}$

The subscript σ_x in equation (8) depends on x as being determined by the sign of difference $x - x_T$: $\sigma_x = +$ for $x > x_T$ and $\sigma_x = -$ for $x < x_T$. The functions $Y(z)$ and $U_\pm(z)$ in equation (8) can be easily computed for a given profile $h(x)$ (or $y(z)$) either analytically (see table 1) or numerically. For instance, in the simplest case of the rectangular domain, $h_\pm(x) = \pm h_0/2$, we get

$$T(x) = \begin{cases} \dfrac{x_T^2 - x^2}{2D} + \dfrac{l}{\kappa} & (0 \leqslant x \leqslant x_T), \\ \dfrac{(x-x_T)(2l-x_T-x)}{2D} + \dfrac{l}{\kappa} & (x_T \leqslant x \leqslant l), \end{cases} \tag{11}$$

Other examples are summarised in table 1 and presented below.

The explicit equation (8) constitutes the main result of the paper and includes two terms. The first (diffusion) term is independent of the size of the target and is related to the time required for a Brownian particle to arrive at the proximity to the target from its starting position. For this reason, the contribution of this term is small when $x \approx x_T$, i.e. when the particle initial position is near the target. The second (reaction) term in equation (8) describes the particle absorption by the target when the particle starts in its vicinity. This term diverges logarithmically as the target size decreases and thus dominates in the small target limit.

We outline that equation (8) is also applicable when the small target is located on the boundary of the domain, i.e., for the so-called narrow escape problem [9, 10, 29–36]. In this case, the equivalent absorbing interval is attached to the boundary and its length is simply a half length of the absorbing interval located on the boundary. The latter statement can be easily deduced by recalling the expression for the conformal radius of an ellipse discussed in section 1 and conceptualising the absorbing interval on the boundary as a half-ellipse with infinitesimal height (see also [12]). This observation also clarifies why the target should be located relatively far from the boundary in the above analysis. In fact, when the target approaches the boundary by a distance smaller than by the target size, the length of the effective absorbing interval becomes somewhat between $2r_c$ (the target is on the boundary) and $4r_c$ (the target is far from the boundary). As the prefactor in front of r_c exhibits a sophisticated dependence on the geometric setting, the related uncertainty does not allow to accurately estimate the trapping rate and thus the mean first-passage time. Qualitatively, such a strong dependence of the trapping rate on the distance to the boundary stems from the diffusion screening of a part of the target, which is oriented towards the boundary. In other words, this part is less accessible to diffusing particles [52–54].

In many applications, the starting point is not fixed but uniformly distributed inside the domain. In this setting, one often resorts to the surface-averaged MFPT:

$$\overline{T} = \frac{1}{S}\int_\Omega \mathrm{d}x\mathrm{d}y\, T(x,y). \tag{12}$$

Substituting our approximate solution (8), we get an explicit approximation for $\overline{T}$:

$$\overline{T}_{\mathrm{app}} = \frac{l^2}{D}\int_0^1 \mathrm{d}z\, \frac{y(z)}{Y(1)}\left(U_{\sigma_{zl}}(z_T) - U_{\sigma_{zl}}(zl)\right) + \frac{l}{\kappa}\frac{Y(1)}{y(z_T)}, \tag{13}$$

where $z_T = x_T/l$. The last integral can be evaluated by using equation (10). After elementary but lengthy computations, we get

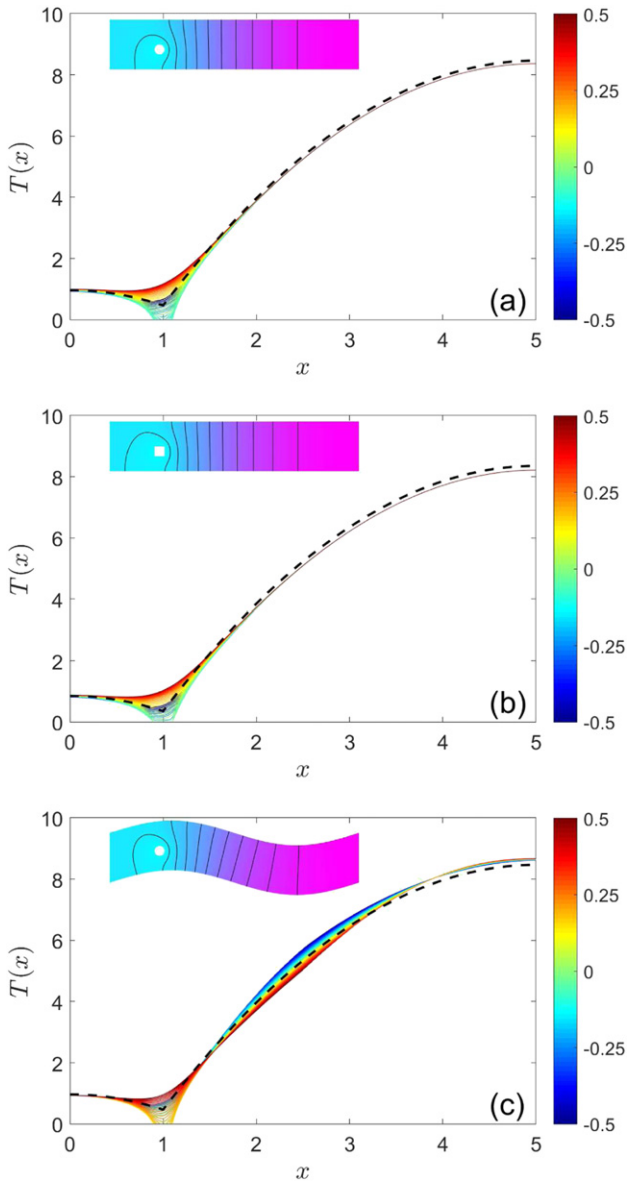

Figure 2. (a) and (b) MFPT to a circular target of radius $\rho = 0.1$ (a) and to a square target with edge length $a = 0.2$ (b), which is located at $(1, -0.1)$ inside an elongated rectangle $(0, 5) \times (-\frac{1}{2}, \frac{1}{2})$ with reflecting boundary, with $D = 1$. Comparison between our approximation (11) (shown by black dashed line) and the FEM solution (coloured lines) as a function of x for 64 equally spaced y, from $y = -\frac{1}{2}$ (dark blue) to $y = \frac{1}{2}$ (dark red). Inset shows the FEM solution $T(x, y)$ as coloured contour plots. (c) MFPT to a circular target of radius $\rho = 0.1$ located at $(1, 0.1378)$ inside a channel with oscillating profile $h_- = -0.5 + 0.25\sin(2\pi x/l)$ and $h_+ = h_- + 1$ of length $l = 5$ and constant height $h = 1$.

$$\overline{T}_{\rm app} = \frac{l^2}{D}\left(U_-(z_T) + U_+(z_T) - C_y\right) + \frac{l}{\kappa}\frac{Y(1)}{y(z_T)}, \tag{14}$$

where

$$C_y = \int_0^1 {\rm d}z\, \frac{Y(z)(Y(1) - Y(z))}{Y(1)y(z)} \tag{15}$$

is the shape-dependent constant.

3. Conditions of validity

The main conditions that limit the range of validity of the proposed approximation come from the two underlying assumptions: (i) a relative smallness of the target with respect to all dimensions of the system ($s/h(x_T) \ll 1$), and (ii) introduction of the effective trapping rate that can adequately characterise the target. The effective trapping rate will be formed at some distance from the target (since near the target it varies at much smaller scale $\sim s \ll h(x_T)$) and this imposes some restriction on the elongation of the

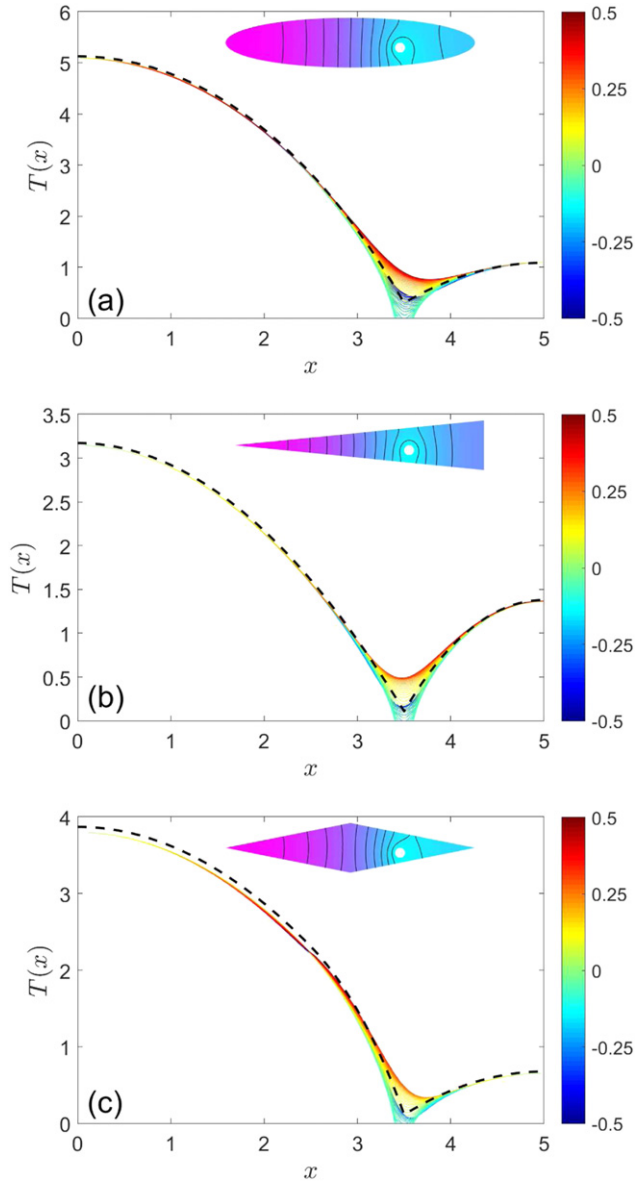

Figure 3. MFPT (obtained by FEM), $T(x, y)$, to a circular target of radius $\rho = 0.1$ inside an elongated domain with reflecting boundary, inserted into a rectangle $(0, 5) \times (-\frac{1}{2}, \frac{1}{2})$, with $D = 1$ and $(x_T, y_T) = (3.5, -0.1)$. (a) Ellipse; (b) triangle; (c) rhombus. 64 coloured curves represent $T(x, y)$ as a function of x for 64 equally spaced y, from $y = -\frac{1}{2}$ (dark blue) to $y = \frac{1}{2}$ (dark red). Black dashed line shows the approximate solution (8), with explicitly found functions $Y(z)$ and $U_{\pm}(z)$ in Table I. Inset shows $T(x, y)$ inside each domain.

domain, as well as on the relative position of the starting point of the particle (e.g., the approximation may be inaccurate if the starting position is in the same cross-section as the target). In line with the previous studies [11], this approximation is expected to provide reasonable estimations of the MFPT even when the target is not infinitesimally small and the longitudinal separation between the starting point of the particle and the target is of the order of the domain height.

As discussed earlier, another minor (geometrical) constraint is related to the proximity of the target to the reflecting boundary. If the distance between the target and the boundary is smaller than the half-length $s/2$ of the equivalent absorbing interval, the result will be indistinguishable from the scenario when the target is touching the boundary. Since we assume that the target is relatively small, $s/h \ll 1$, this limitation is insignificant.

Finally, as we neglect the curvature effect onto diffusivity, the profiles $h_{\pm}(x)$ of the domain boundary should vary smoothly, which can be expressed by assuming that $\max_x\{|h'_{\pm}(x)|\}$ is a small parameter [45].

More quantitative criteria for the validity of the proposed framework will be established below by numerical simulations.

Table 2. The surface-averaged MFPT, $\overline{T}$, estimated from the numerical solution of the original problem (solved by a FEM), and its explicit approximation $\overline{T}_{\rm app}$ from equation (14), for five examples shown in figures 2 and 3.

Domain	$\overline{T}$	$\overline{T}_{\rm app}$	Relative error
Rectangular (circle)	4.7481	4.7961	1%
Rectangular (square)	4.6128	4.6855	2%
Triangular	1.5567	1.5522	0.3%
Rhombic	1.2096	1.1888	2%
Elliptic	4.0403	4.0340	0.2%

4. Numerical simulations

We validate our analytical approximation for the MFPT, equation (8), by comparison with the results of a direct numerical solution of the boundary value problem (1) by means of a finite element method (FEM) solver implemented in Matlab PDEtool. First, we calculated MFPT in the rectangular domain for a circular target of radius ρ, so the length of the equivalent absorbing interval is $s = 4\rho$. Figure 2(a) shows the MFPT, $T(x, y)$, for a circular target of radius $\rho = 0.1$ located at $(1, -0.1)$ inside an elongated rectangle $\Omega = (0, 5) \times (-\frac{1}{2}, \frac{1}{2})$ with reflecting boundary (i.e., $l = 5$ and $h_0 = 1$). In line with the above comments, our analytical approximation provides good estimates of the MFPT, except for the cases when the initial position of the particle is very close to the target (less than h_0). This condition provides a quantitative criterion for applicability of this analytical framework.

Next we analyse the effect of the target shape on the MFPT. To this end we consider the MFPT to a small absorbing square of side a in the same rectangular domain, for which the length of the equivalent absorbing interval is $s = a\Gamma^2(1/4)/\pi^{3/2} \approx 2.36a$. Figure 2(b) shows a good agreement between our approximation and the FEM solution for a square of side $a = 0.2$ at the same location inside the same rectangle as in figure 2(a). One can see that the target shape is correctly captured via its conformal radius.

As the shape of the elongated domain enters into the Fick-Jacobs equation (5) only through the height $h(x) = h_+(x) - h_-(x)$, our approximation (8) predicts the *same* MFPT for different domains, for which the function $h(x)$ remains unchanged. In particular, one gets the explicit solution (11) for any channel of a constant height. In order to test the validity of such an approximation, we compute the MFPT to a circular target inside a channel with an oscillating profile $h_-(x) = -0.5 + c\sin(2\pi\omega x/l)$ and $h_+(x) = h_-(x) + 1$. Figure 2(c) shows good agreement for $c = 0.25$ and $\omega = 1$, even though the numerical curves $T(x, y)$ corresponding to different y exhibit broader fluctuations even at large distances from the target. If the amplitude c or the frequency ω of oscillations of the channel profile increase, the curvilinear distance between the target and the starting point increases and so does the MFPT. For instance, at $c = 1$, the approximation (11) underestimates the MFPT by 35% at the most distant starting point (figure not shown). A conventional way of improving the approximation is to account for the next order in the perturbation expansion, which entails introduction of the position-dependent diffusion coefficient via the substitution [46]

$$D \to \frac{D}{\left(1 + \frac{1}{4}[h'(x)]^2\right)^{1/3}}, \tag{16}$$

where $h'(x) = {\rm d}h/{\rm d}x$. However, if the width of the domain $h(x)$ is constant (as in the example in figure 2(c)), then equation (16) gives back a constant diffusivity, and the next order in the perturbation expansion should be accounted directly in equation (5).

To validate the proposed framework for other elongated domains we calculated the MFPT in three domains of different shape (an ellipse, a triangle, and a rhombus), for which we kept the same aspect ratio as before: $h_0/l = 0.2$. A circular target of radius $\rho = 0.1$ is located at the same position inside these domains. Figure 3 illustrates an excellent agreement between our approximation in equation (8) and numerical solutions for all these domains. We also checked that the relative error of the explicit approximation (14) for the surface-averaged MFPT, $\overline{T}$, does not exceed 2% for all these examples (see table 2).

5. Conclusion

We obtained a simple formula (8) for the MFPT to a small absorbing target of an arbitrary shape in an elongated planar domain with slowly changing boundary profile. This formula expresses MFPT in terms of dimensions of the domain, the form and size of the absorbing target and its relative position inside the

domain. We validated our analytical predictions by numerical simulations and found excellent agreement. Indeed, if the initial position of the particle and the target location are well separated (more than half of the height of the domain at the target location x_T) then the numerical and analytical results are almost indistinguishable; but even for closer separations the analytical predictions are still reasonable, see figures 2 and 3. The proposed expression for the MFPT is a useful tool for some rapid practical estimations as well as for validation of complex numerical models of particle diffusion in geometrically constrained settings.

Future work may involve an extension of the proposed framework to more complex geometries (an elongated domain with an arbitrary piecewise boundary) or an extension to the three-dimensional settings. In particular, the Fick–Jacobs equation (5) remains applicable in three dimensions, if $h(x)$ denotes the cross-sectional area of the domain, while the main challenge consists in finding an appropriate expression for the trapping rate of the target, i.e., a 3D generalisation of equation (3).

Acknowledgments

DSG acknowledges a partial financial support from the Alexander von Humboldt Foundation through a Bessel Research Award. ATS thanks Alexander M Berezhkovskii and Paul A Martin for many helpful discussions.

ORCID iDs

Denis S. Grebenkov https://orcid.org/0000-0002-6273-9164
Alexei T. Skvortsov https://orcid.org/0000-0001-8202-7052

References

[1] Redner S 2001 *Guide to First Passage Processes* (Cambridge: Cambridge University Press)
[2] Bray A J, Majumdar S N and Schehr G 2013 Persistence and first-passage properties in nonequilibrium systems *Adv. Phys.* **62** 225–361
[3] Metzler R, Oshanin G and Redner S (ed) 2014 *First-Passage Phenomena and Their Applications* (Singapore: World Scientific)
[4] Bénichou O and Voituriez R 2014 From first-passage times of random walks in confinement to geometry-controlled kinetics *Phys. Rep.* **539** 225–84
[5] Bressloff P and Lawley S D 2015 Stochastically gated diffusion-limited reactions for a small target in a bounded domain *Phys. Rev.* E **92** 062117
[6] Lindenberg K, Metzler R and Oshanin G (ed) 2019 *Chemical Kinetics: Beyond the Textbook* (Singapore: World Scientific)
[7] Oshanin G, Vasilyev O, Krapivsky P L and Klafter J 2009 Survival of an evasive prey *Proc. Natl Acad. Sci.* **106** 13696–701
[8] Lindsay A E, Bernoff A J and Ward M J 2017 First passage statistics for the capture of a Brownian particle by a structured spherical target with multiple surface traps *Multiscale Model. Simul.* **15** 74–109
[9] Holcman D and Schuss Z 2015 *Stochastic Narrow Escape in Molecular and Cellular Biology* (Berlin: Springer)
[10] Grebenkov D S 2016 Universal formula for the mean first passage time in planar domains *Phys. Rev. Lett.* **117** 260201
[11] Dagdug L, Berezhkovskii A M and Skvortsov A T 2015 Trapping of diffusing particles by striped cylindrical surfaces. Boundary homogenization approach *J. Chem. Phys.* **142** 234902
[12] Skvortsov A T, Berezhkovskii A M and Dagdug L 2018 Trapping of diffusing particles by spiky absorbers *J. Chem. Phys.* **148** 084103
[13] Skvortsov A T 2020 Mean first passage time for a particle diffusing on a disk with two absorbing traps at the boundary *Phys. Rev.* E **102** 012123
[14] Grebenkov D S 2020 Paradigm shift in diffusion-mediated surface phenomena *Phys. Rev. Lett.* **125** 078102
[15] Grebenkov D S 2019 Imperfect diffusion-controlled reactions *Chemical Kinetics: Beyond the Textbook* ed K Lindenberg, R Metzler and G Oshanin (Singapore: World Scientific) ch 8 pp 191–219
[16] Bazant M Z 2016 Exact solutions and physical analogies for unidirectional flows *Phys. Rev. Fluids* **1** 024001
[17] Mattos T, Mejía-Monasterio C, Metzler R and Oshanin G 2012 First passages in bounded domains: when is the mean first passage time meaningful? *Phys. Rev.* E **86** 031143
[18] Rupprecht J-F, Bénichou O, Grebenkov D S and Voituriez R 2015 Exit time distribution in spherically symmetric two-dimensional domains *J. Stat. Phys.* **158** 192–230
[19] Godec A and Metzler R 2016 Universal proximity effect in target search kinetics in the few encounter limit *Phys. Rev.* X **6** 041037
[20] Godec A and Metzler R 2016 First passage time distribution in heterogeneity controlled kinetics: going beyond the mean first passage time *Sci. Rep.* **6** 20349
[21] Lanoiselée Y, Moutal N and Grebenkov D S 2018 Diffusion-limited reactions in dynamic heterogeneous media *Nat. Commun.* **9** 4398
[22] Grebenkov D S, Metzler R and Oshanin G 2018 Towards a full quantitative description of single-molecule reaction kinetics in biological cells *Phys. Chem. Chem. Phys.* **20** 16393–401
[23] Grebenkov D S, Metzler R and Oshanin G 2018 Strong defocusing of molecular reaction times results from an interplay of geometry and reaction control *Commun. Chem.* **1** 96
[24] Grebenkov D S, Metzler R and Oshanin G 2019 Full distribution of first exit times in the narrow escape problem *New J. Phys.* **21** 122001

[25] Condamin S, Bénichou O, Tejedor V, Voituriez R and Klafter J 2007 First-passage times in complex scale-invariant media *Nature* **450** 77–80
[26] Bénichou O and Voituriez R 2008 Narrow-escape time problem: time needed for a particle to exit a confining domain through a small window *Phys. Rev. Lett.* **100** 168105
[27] Bénichou O, Chevalier C, Klafter J, Meyer B and Voituriez R 2010 Geometry-controlled kinetics *Nat. Chem.* **2** 472–7
[28] Guérin T, Levernier N, Bénichou O and Voituriez R 2016 Mean first-passage times of non-Markovian random walkers in confinement *Nature* **534** 356–9
[29] Singer A, Schuss Z, Holcman D and Eisenberg R S 2006 Narrow escape: Part I *J. Stat. Phys.* **122** 437–63
[30] Singer A, Schuss Z and Holcman D 2006 Narrow escape: Part II. The circular disk *J. Stat. Phys.* **122** 465
[31] Singer A, Schuss Z and Holcman D 2006 Narrow escape: Part III. Non-smooth domains and Riemann surfaces *J. Stat. Phys.* **122** 491
[32] Pillay S, Ward M J, Peirce A and Kolokolnikov T 2010 An asymptotic analysis of the mean first passage time for narrow escape problems: Part I. Two-dimensional domains *Multiscale Model. Simul.* **8** 803–35
[33] Cheviakov A F, Ward M J and Straube R 2010 An asymptotic analysis of the mean first passage time for narrow escape problems: Part II. The sphere *Multiscale Model. Simul.* **8** 836–70
[34] Cheviakov A F, Reimer A S and Ward M J 2012 Mathematical modeling and numerical computation of narrow escape problems *Phys. Rev.* E **85** 021131
[35] Caginalp C and Chen X 2012 Analytical and numerical results for an escape problem *Arch. Ration. Mech. Anal.* **203** 329–42
[36] Marshall J S 2016 Analytical solutions for an escape problem in a disc with an arbitrary distribution of exit holes along its boundary *J. Stat. Phys.* **165** 920–52
[37] Iyaniwura S A, Wong T, Macdonald C B and Ward M J 2020 Optimization of the mean first passage time in near-disk and elliptical domains in 2-D with small absorbing traps (arXiv:2006.12722)
[38] Landkof N 1972 *Foundations of Modern Potential Theory* (Berlin: Springer)
[39] Ransford T and Rostand J 2007 Computation of capacity *Math. Comp.* **76** 1499–521
[40] Ransford T 2010 Computation of logarithmic capacity *Comput. Methods Funct. Theory* **10** 555–78
[41] Crocker M J 1998 *Handbook of Acoustics* (New York: Wiley)
[42] Tretyakov S 2003 *Analytical Modeling in Applied Electromagnetics* (Boston, MA: Artech)
[43] Hewett D P and Hewitt I J 2016 Homogenized boundary conditions and resonance effects in Faraday cages *Proc. R. Soc.* A **472** 20160062
[44] Marigo J-J and Maurel A 2016 Two-scale homogenization to determine effective parameters of thin metallic-structured films *Proc. R. Soc.* A **472** 20160068
[45] Zwanzig R 1992 Diffusion past an entropy barrier *J. Phys. Chem.* **96** 3926–30
[46] Reguera D and Rubi J M 2001 Kinetic equations for diffusion in the presence of entropic barriers *Phys. Rev.* E **64** 061106
[47] Kalinay P and Percus J K 2006 Corrections to the Fick–Jacobs equation *Phys. Rev.* E **74** 041203
[48] Bradley R M 2009 Diffusion in a two-dimensional channel with curved midline and varying width: reduction to an effective one-dimensional description *Phys. Rev.* E **80** 061142
[49] Rubi J M and Reguera D 2010 Thermodynamics and stochastic dynamics of transport in confined media *Chem. Phys.* **375** 518–22
[50] Dagdug L, Vazquez M-V, Berezhkovskii A M, Zitserman V Y and Bezrukov S M 2012 Diffusion in the presence of cylindrical obstacles arranged in a square lattice analyzed with generalized Fick–Jacobs equation *J. Chem. Phys.* **136** 204106
[51] Gardiner C W 1985 *Handbook of Stochastic Methods for Physics, Chemistry and the Natural Sciences* (Berlin: Springer)
[52] Felici M, Filoche M and Sapoval B 2003 Diffusional screening in the human pulmonary acinus *J. Appl. Physiol.* **94** 2010
[53] Grebenkov D S 2005 What makes a boundary less accessible *Phys. Rev. Lett.* **95** 200602
[54] Andrade J S Jr, Araújo A D, Filoche M and Sapoval B 2007 Screening effects in flow through rough channels *Phys. Rev. Lett.* **98** 194101